POLITECNICO DI TORINO
Repository ISTITUZIONALE

Proposal of a coast-down model including speed dependent coefficients for the retarding forces

(Article begins on next page)

27 April 2024

Proposal of a coast-down model including speed dependent coefficients for the retarding forces

Paolo Baldissera

Abstract

Coast-down techniques are widely used on bicycles and motorized vehicles in order to estimate retarding forces and respective coefficients. The mathematical model behind coast-down data analysis is usually based on the assumption that both drag and rolling-resistance coefficients do not depend on the vehicle speed. This assumption restricts the model validity to the specifically tested range of speeds and provide averaged values for the force coefficients. In the attempt to overcome this limitation, the proposal of a complete polynomial equation of motion is developed, evaluated and discussed through a human-powered vehicle case study. The analysis points out that the extended model is adequate for experimental data fitting and could potentially provide a more reliable power-speed prediction outside the testing range. However, the expressions included in the model in order to account for speed-dependent coefficients is a first approximation with limited capability to represent these complex phenomena. As a consequence, further experimental testing is needed in order to achieve a validation. Advantages and side effects of both the classical and the complete polynomial models are discussed, concluding that the two approaches could be complementary and could answer different needs that specifically depend on the purpose of the coast-down analysis.

Introduction

The coast-down is a quite popular method to assess the performance of bicycles and Human Powered Vehicles (HPVs). The procedure consists of letting the vehicle slow down through a specific range of speeds in order to estimate the resistive forces for the assumed physical model. The selected road segment has to be flat or at least with a known slight and constant slope. The road surface must be regular with no bumps and holes. Since the wind can strongly affect the results, the ideal proving ground is an indoor track. However, open-air measurements are possible with a steady wind up to 4-5 km/h in speed, by measuring it in order to correct acquired data.

Coast-down techniques can be used at different levels of accuracy and complexity depending on the available data-logging tools and post-processing capabilities. These methods have been used to assess performance of bicycles[1–5] and wheelchairs[6;7] and can be potentially applied to every sport involving rolling or even sliding on a surface, after proper adaptation of the model. Similar approaches based on deceleration measurement have been applied also to swimming[8], ice skating[9] and bobsleighing[10]. At the industrial level, the automotive industries make a wide use of such kinds of tests[11–14] that are also defined by SAE (Society of Automotive Engineers) Recommended Practices[15;16] and combined with laboratory and wind tunnel results[17].

The equation of motion

A coast-down procedure involves the logging of speed and time data in order to obtain a quantitative estimation of all the resistive forces through the application of a mathematical model. The full equation of motion has to be considered, and the choice of the correct model plays a crucial role in the following.

The equation of motion for a freewheeling cyclist has been largely discussed and analyzed in literature[3–5;7;18–21] and can be summarized in its simplest form as:

$$m \cdot \frac{dv}{dt} = -F_r - F_d \qquad (1)$$

where F_r and F_d are the rolling-resistance and the air-drag forces respectively acting against the vehicle.

By definition of the drag coefficient C_d, the aerodynamic force F_d can be expressed black as:

$$F_d = \frac{1}{2} \cdot \rho \cdot C_d \cdot A \cdot v^2 = K_d \cdot v^2 \qquad (2)$$

where ρ is the air density, A is the frontal area and K_d is the aerodynamic drag factor.

By definition of the rolling-resistance coefficient C_{rr}, the rolling-resistance force F_r can be expressed as a function of the normal load N:

$$F_r = C_{rr} \cdot N. \qquad (3)$$

Politecnico di Torino, Torino, Italy

Corresponding author:
Paolo Baldissera Politecnico di Torino, Corso Duca degli Abruzzi, 24, 10129 Torino, Italy.
Email: paolo.baldissera@polito.it

It must be noted that F_r includes not only the tire rolling-resistance, but also a contribution from the wheel hub bearings.

If the aerodynamic lift forces are negligible, the normal load N corresponds to the weight of the vehicle plus rider.

The overall equation of motion can be summarized in:

$$m \cdot \frac{dv}{dt} = -C_{rr} \cdot N - \frac{1}{2} \cdot \rho \cdot C_d \cdot A \cdot v^2. \qquad (4)$$

From this expression multiplied by the speed, it is possible to obtain the power required at the wheel P_w, which is the mechanical power at the pedals P_p reduced by the transmission efficiency η:

$$P_w = \eta \cdot P_p = -C_{rr} \cdot N \cdot v - \frac{1}{2} \cdot \rho \cdot C_d \cdot A \cdot v^3. \qquad (5)$$

The pure quadratic model

Under the assumption that both C_{rr} and C_d (and thus F_r and K_d) do not depend on the speed, Eq. (4) is defined as a first-order pure quadratic differential equation and it has the closed-form solution reported by Hennekam and Govers[4;5]:

$$v(t) = \beta \cdot \tan\left(\phi - \frac{t}{\tau}\right) \qquad (6)$$

where ϕ is obtained by imposing the initial speed v_0 for the time $t = 0$:

$$\phi = \arctan\frac{v_0}{\beta}. \qquad (7)$$

By estimating the parameters β and τ through experimental data fitting, it can be finally obtained:

$$\begin{cases} F_r = \dfrac{m \cdot \beta}{\tau} \\[3mm] K_d = \dfrac{m}{\beta \cdot \tau}. \end{cases} \qquad (8)$$

In the following, this model and its solution will be referenced as PQ (pure quadratic).

It is likely that the above-mentioned assumption is acceptable when fitting data for bicycles in their typical range of speeds. However, when the purpose is to obtain a predictive model of the power required at speeds beyond the range of testing, some caution should be used before relying on a PQ model. If K_d and F_r are not really constant, but depend on the speed, the values estimated by the PQ model will represent some sort of average within the experimental range of velocities. This implies that the estimated coefficients will depend on the selected range of speeds and any prediction outside this range will be affected by such approximation. Moreover, the further the target speed is far from the experimental range, the more the prediction error will be increased. Finally, any accurate comparison among different vehicles and/or configurations will be possible only with C_d and C_{rr} values that were derived from a similar range of testing speeds.

The need for a predictive model

The need for a predictive model is often occurring with top-speed HPVs due to significant differences between racing

and testing conditions. In particular, this class of machines includes the streamlined vehicles yearly attending the World Human Powered Speed Championship[22;23] (WHPSC) in Battle Mountain (Nevada, US) with the purpose of reaching top speeds at the end of a quite flat segment (average slope -0.6%) of 8 km length on the State Route 305. Pushing the cycling technology beyond the limit of the Unione Cycliste Internationale (UCI) rules, this competition offers an ideal framework for engineering education and stimulates the frontier research on HPVs[24;25], as confirmed by the regular presence of university teams. Since it is unlikely for the participants to have a proving ground with the quite ideal conditions of the SR305, all training and testing is usually limited to speeds up to 90-100 km/h. However, there is a need to predict the power required for much higher velocity. Indeed, the world speed record was broken at 139.45 km/h in September 2015 by the Canadian rider Todd Reichert on the prototype Eta[26] (Aerovelo Team).

The complete polynomial model

As observed before, the typical literature model for bicycle coast-down is a PQ expression, which means it has no linear terms or, in other words, it is an incomplete quadratic polynomial. In the context of a specific case study, it was in the interest of the author to verify if speed dependent C_d and/or C_{rr} could be estimated by using a complete polynomial model (CP) for the equation of motion.

A quadratic CP model has the following general form:

$$m \cdot \frac{dv}{dt} = -a - b \cdot v - c \cdot v^2. \qquad (9)$$

The solution of Eq. (9) will be discussed and developed in the following section.

Mathematical solution of the CP model for the equation of motion

Eq. (9) has a closed form solution in the form:

$$v(t) = \frac{d \cdot \tan\left[\dfrac{1}{2}\left(k \cdot d - \dfrac{t}{m} \cdot d\right)\right] - b}{2c} \qquad (10)$$

where

$$d = \sqrt{4ac - b^2}, \qquad (11)$$

Eq. (10) can be rewritten as:

$$v(t) = \beta \cdot \tan\left(\phi - \frac{t}{\tau}\right) - \delta \qquad (12)$$

where

$$\begin{cases} \beta = \dfrac{d}{2c} \\[3mm] \tau = \dfrac{2m}{d} \\[3mm] \delta = \dfrac{b}{2c} \\[3mm] \phi = \dfrac{k \cdot m}{\tau} = \arctan\dfrac{v_0 + \delta}{\beta}. \end{cases} \qquad (13)$$

As for the PQ model, the phase factor ϕ is determined by imposing the initial speed condition at $t = 0$:

$$v(0) = v_0 = \beta \cdot \tan \phi - \delta. \quad (14)$$

Finally, the polynomial coefficients can be expressed as a function of the mass and of the fitting parameters β, δ and τ:

$$\begin{cases} a = \dfrac{m \cdot (\beta^2 + \delta^2)}{\beta \cdot \tau} \\[2mm] b = \dfrac{2 \cdot m \cdot \delta}{\beta \cdot \tau} \\[2mm] c = \dfrac{m}{\beta \cdot \tau}. \end{cases} \quad (15)$$

The obtained solution looks very similar to the PQ one, with the only apparent difference being in the term δ. In fact, Eq. (12) is a more general solution that includes Eq. (4). It can be verified that the factors expressed in Eq. (15) reduce to the ones of the PQ model[4;5] when $b = 0 \Rightarrow \delta = 0$.

The physics behind the CP model

With the mathematical solution of the CP model now available for data fitting, it is important to clarify the physical meaning that each estimated parameter could have, with particular focus on the newly introduced linear term in Eq. (9).

In the following, three physical phenomena are assumed as potential sources of the linear term:

1. a linear dependence on the speed for the freehub mechanical losses;
2. a linear dependence on the speed for C_{rr};
3. an inverse linear dependence on the speed for C_d.

Concerning the first phenomenon, it must be noted that, during the coast-down procedure, the rider stops pedaling and the chain is not moving. Under this condition, the freehub plays its role by letting the wheel rotate independently from the cassette sprockets. Freehub mechanisms are available in the market in a wide range of prices and quality levels. A resistive force contribution arising from the freehub is certainly present in every bicycle and HPV, and it is possible that it linearly depends on the speed, as typically happens with transmission mechanical losses.

The dependence on speed for the rolling-resistance coefficient is often reported by automotive[27;28] and cycling[29] literature, but with a lack of experimental data. In one experimental case[30], both the linear and the quadratic dependencies of C_{rr} on the speed appeared to be negligible, at least for the limited range of speed of the specific case.

Finally, dependence on the speed for the drag coefficient is a well-known phenomenon, often reported in literature[24;31;32] by plotting C_d as a function of the Reynolds number Re, defined as:

$$Re = \frac{v \cdot l}{\nu} \quad (16)$$

where l is the length of the body and ν is the air kinematic viscosity ($1.5111 \cdot 10^{-5}$ at 20 °C).

Actually, the relationship between C_d and Re is not usually representable by means of specific mathematical laws on a large scale. In fact, it is a complex behaviour that can show rapid changes and critical transition zones between different flow regimes. However, considering that an inverse linear trend should be a better approximation than fully neglecting a true dependence on the speed, this simple relationship will be introduced in the model and discussed again later.

In order to have these phenomena contributing to the linear term of the CP model, the retarding forces can be mathematically expressed as:

$$\begin{cases} F_{hub} = f_h \cdot v \\ F_r = F_{r0} + F_{rv} = F_{r0} + f_{rv} \cdot v \\ F_d = F_{dv1} + F_{dv2} = k_{d1} \cdot v + K_{d2} \cdot v^2 \end{cases} \quad (17)$$

where:

$$\begin{cases} F_{r0} = C_{r0} \cdot N \\ f_{rv} = c_{rv} \cdot N \\ C_{rr} = C_{r0} + c_{rv} \cdot v \end{cases} \quad (18)$$

and:

$$\begin{cases} k_{d1} = \dfrac{1}{2} \cdot \rho \cdot A \cdot c_{dv} \\[2mm] K_{d2} = \dfrac{1}{2} \cdot \rho \cdot A \cdot C_{d0} \\[2mm] C_d = C_{d0} + \dfrac{c_{dv}}{v}. \end{cases} \quad (19)$$

Finally, the CP equation of motion including all these contributions has the following form:

$$m \cdot \frac{dv}{dt} = -F_{r0} - (f_h + f_{rv} + k_{d1}) \cdot v - K_{d2} \cdot v^2 \quad (20)$$

.

As a consequence, by comparison with Eq. (9):

$$\begin{cases} a = F_{r0} \\[2mm] b = f_h + f_{rv} + k_{d1} \\[2mm] c = K_{d2}. \end{cases} \quad (21)$$

It is important to point out that the presence of combined phenomena in the expression of b changes the perspective in which the model results have to be interpreted. With the CP model it will be still possible to plot each term contribution to the required power, but it will not be possible to quantify rolling-resistance and air-drag separately. Only under specific conditions, it will be possible to distinguish these contributions:

1. when the speed dependence of two terms over three have been already assessed through other tests; or
2. when it has been verified that one of them is largely dominating while the two others are negligible.

In all other cases, it will be impossible to separate these contributions, and the only way to compare different vehicles or configurations will be through plotting of power-speed curves.

In the following, the PQ and CP models will be applied and compared through a case study in order to evaluate differences in their fitting capabilities and in their predictive behaviour.

Case study application

During the WHPSC 2015, a student team coordinated by the authors had its debut and set the national Italian record at 116.19 km/h. After designing and manufacturing the prototype (PulsaR, Figure 1), the coast-down method was largely used in order to assess the vehicle performance. This provided the opportunity to examine the methodology and to develop the work presented in this paper.

Figure 1. PulsaR, the HPV prototype of the Policumbent Student Team at Politecnico di Torino.

Testing setup and procedure

The testing was performed on a 7.8 km long circuit. Since the track is generally used for trucks, the road asphalt surface is quite rough, but regular in slope ($\leq 0.1\%$) and with no bumps in the selected straight segment of about 3 km.

The speed data were logged through a rear-wheel magnet and Hall sensor connected to an Arduino UNO micro-controller as shown in Figure 2. The controller checks for the presence of the magnet at a frequency of 60 Hz. With each two consecutive passages of the magnet, the controller calculates the rotational speed considering the tire metric development (measured on the road with the rider on the vehicle) and with a preselected resolution of 0.001 m/s. As a consequence, the acquired data do not have a fixed resolution in time, but in space, corresponding to the circumference of the rear wheel.

The overall prototype plus rider mass was 91 kg, strongly unbalanced towards the front wheel, that was supporting 60 kg (66% of the total). A frontal area of 0.259 m^2 was estimated from 3D CAD drawings. An overall length of 2.78 m was measured for the vehicle.

The rider performed three coast-down repetitions on the same segment of the track. The target speed range was from 20 to 5 m/s (72-18 km/h), but data for the fitting were selected between 19.0 and 6.0 m/s (68.4-21.6 km/h) according to the minimum common range effectively obtained.

Air conditions were measured with a Kestrel 3500 portable weather station: temperature, pressure and relative humidity were registered at each run during the test as far as the wind speed average and peak in the direction of motion. A maximum wind peak of 0.8 m/s was registered and average values of the three repetitions were of 0.0, 0.5 and 0.7 m/s, respectively, with a good alignment to the direction of motion. The average wind speed for each run was then subtracted from the measured vehicle speed. This operation does not fully remove the error, but rather moves it to the
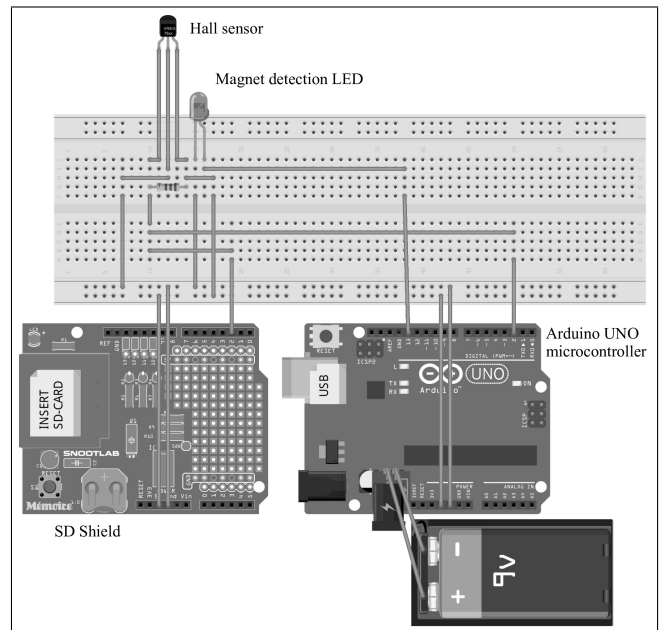

Figure 2. Scheme of the logger system.

ground relative speed and the rolling-resistance estimation. Since the purpose was to obtain a model for power prediction beyond the testing range of speeds, it has been considered acceptable to move this error to the relative minor contributor in order to have a more accurate estimation on the air-drag. Average temperature was 19.2 °C, with 1007.1 hPa of pressure and 53.1% relative humidity, resulting in an approximated air density $\rho = 1.1946$ kg/m^3.

Data fitting and analysis

All three repetitions were shifted in order to start from $t = 0$ at 19 m/s and then aggregated in a single cloud of experimental points to be sorted by ascending values of t. Then, each set was imported into QtiPlot[33] and fitted with both the models (PQ and CP) in order to estimate the parameters β, τ and δ (and then a, b and c).

When fitting experimental data with mathematical expressions, two statistical measurements are especially useful to evaluate and compare alternative models. The first one is the well-known coefficient of determination R^2, which quantify how close the obtained curve is to the experimental data. However, the presence of useless additional parameters in a model can produce an artificial increase of R^2. From this perspective, it becomes rather important to consider the value of another statistical measurement named adjusted-R^2 (or $\bar{R}^2$). By definition[34], $\bar{R}^2$ is lower than R^2 and increases only when the increase of R^2, due to the inclusion of a new parameter, is more than what is expected by chance. In other words, unlike R^2, the value of $\bar{R}^2$ is lowered by the presence of extra parameters that do not improve the model.

In this specific case, if C_d, C_{rr} and F_{hub} are effectively independent from the speed, then data fitting with a CP model is expected to provide the following results:

$$\begin{cases} a \simeq F_r = C_{rr} \cdot N \\ b \simeq 0 \\ c \simeq K_d = \dfrac{1}{2} \cdot \rho \cdot C_d \cdot A \\ \bar{R}^2_{CP} < \bar{R}^2_{PQ}. \end{cases} \qquad (22)$$

Otherwise, in particular if $\bar{R}^2$ is increased for the CP model, it means that the additional term is not useless and the physics behind the phenomenon is more accurately described by its inclusion.

Results and discussion

In Figure 3 the speed vs. time aggregated data are plotted, showing a good repeatability, and fitted with the CP model. The PQ model fitting is omitted in the plot, as it would not be distinguishable from a qualitative point of view in this range of speeds. For a more detailed evaluation, the estimated parameters for the two models are compared in Table 1, including the above-mentioned statistical measurements.
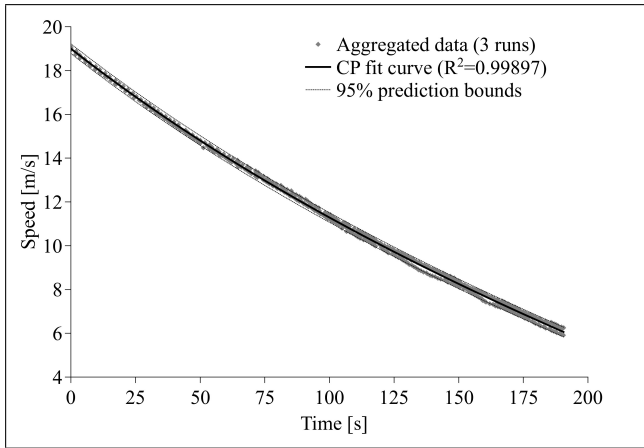

Figure 3. Aggregated data and CP fitting curve with 95% reliability prediction bounds.

Both the parameters a and c are significantly different for the two models, and the value of the parameter b estimated for the CP model cannot be approximated to zero at all. The high R^2 of the PQ model confirms that it is sufficient to adequately approximate the retarding forces in the testing range of speeds. The use of the CP model gives only a marginal improvement to the fitting in such a range, but its slightly higher $\bar{R}^2$ confirms that the additional parameter is not useless. The difference becomes significant when comparing the required power at the wheel versus speed that is predicted by the two models (Figure 4). The two curves significantly overlap below 100 km/h (as a consequence of the fitting procedure below 70 km/h), but they significantly diverge beyond such speed, showing a difference up to 100 W close to the current world record speed.

The role of the new term b can be quantified for the case study by plotting the contribution of each term to the overall power-speed curve (Figure 5). In this case b gives a contribution comparable to the quadratic term (cubic for power) up to 60 km/h and gets closer to the constant term (linear for power) after 100 km/h. It is to be stressed again that in the CP model, unlike the PQ model, none of the terms are self-sufficient to quantify the air-drag or
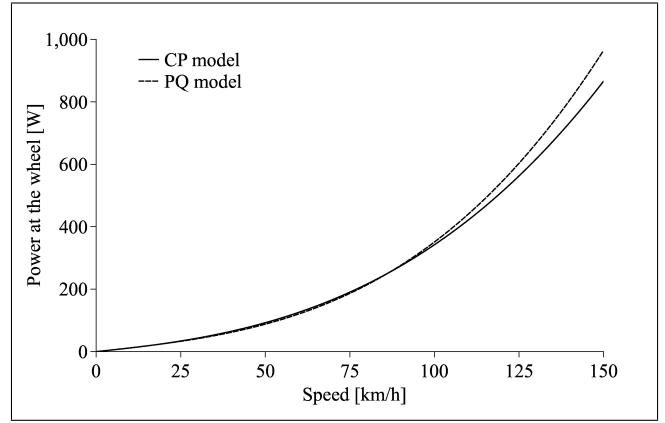

Figure 4. Comparison of the power versus speed curves estimated by the two models.

the rolling-resistance power. Only by keeping in mind this point, it is possible to fully understand Figure 5 and to avoid misunderstandings.
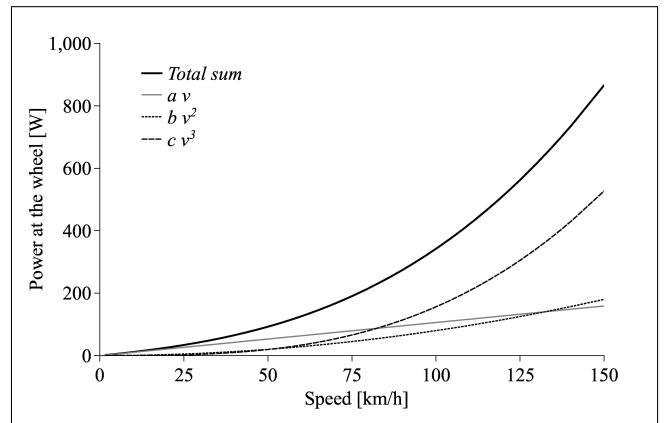

Figure 5. Overall power versus speed and specific contributions from the three terms of the CP model.

In the following, through comparison with literature and simulation data, it will be verified whether the estimated value of b can be addressed to a single contribution among the three of Eq. (21).

Hp.1) Only the freehub losses depend on the speed

Under this hypothesis, it would be:

$$\begin{cases} a = F_{r0} = F_r \\ b = f_{hub} + f_{rv}^{\;0} + k_{d1}^{\;0} \\ c = K_{d2} = K_d. \end{cases} \qquad (23)$$

However, excluding the case of defective components, it is unlikely that the contribution of the freehub can reach the level suggested by Figure 5. Based on the positive experience of over 1000 km training, testing and even racing at the WHPSC with the same prototype, transmission anomalies (i.e. from incorrect assembly or defective components) were excluded in the specific case study. Moreover, under this hypothesis, the air-drag coefficient resulting from the value

Table 1. Fitting parameters with R^2 and $\bar{R}^2$ for the two models.

Model	a	b	c	R^2	$\bar{R}^2$
PQ*	4.218	-	0.01090	0.99896366	0.9989597
CP	3.813	0.1037	0.00728	0.99897128	0.9989654

* $a = F_r$ and $c = K_d$ for the CP model, with reference to Eq. (4)

of c would be 0.047, far below any CFD estimations (details under Hp.3) and not compatible with the obtained top speed at the WHPSC 2015.

This leads to the conclusion that, although the freehub resistance can give a minor contribution to the linear term, it is largely insufficient to justify the estimated value of b. As a consequence, hypothesis 1) is rejected and further investigations should be considered in order to assess if the freehub contribution can be neglected at all.

Hp.2) Only the rolling-resistance coefficient depends on the speed

The second hypothesis is that the linear term is to be fully addressed to the dependence on the speed of the rolling-resistance coefficient Crr, so that:

$$
\begin{cases}
a = F_{r0} \\
b = \cancel{f_{hub}}^{0} + f_{rv} + \cancel{k_{d1}}^{0} \\
c = K_{d2} = K_d.
\end{cases}
\tag{24}
$$

In this case, by using the values of a and b in Table 1, the overall vehicle C_{rr} of Eq. (18) can be plotted as shown in Figure 6. The obtained behaviour looks disproportional
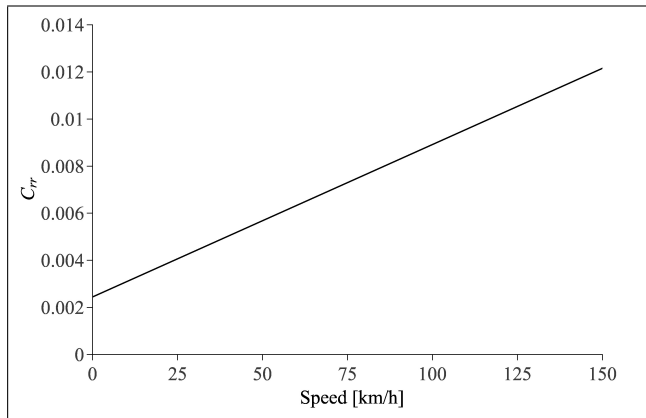

Figure 6. Rolling coefficient versus speed as it would result from Hp.2).

to what could be expected, resulting in a 23% decrease, from 19 to 6 m/s, in the overall rolling-resistance coefficient during the coast-down procedure. Moreover, when projected to world record speeds, the rolling-resistance would double its initial value. Finally, as with the first hypothesis, also in this case the air-drag coefficient obtained by the value of c would be much lower than expected.

This leads to conclude that, although a variation of the rolling-resistance with the speed can partly contribute to the linear term, it does not provide a self-sufficient explanation for it. As a consequence, hypothesis 2) is rejected.

Hp.3) Only the drag coefficient depends on the speed

Under this third hypothesis it would be:

$$
\begin{cases}
a = F_{r0} = F_r \\
b = \cancel{f_{hub}}^{0} + \cancel{f_{rv}}^{0} + k_{d1} \\
c = K_{d2}.
\end{cases}
\tag{25}
$$

Starting from Eq. (16) and Eq. (19), it is possible to write the C_d as a function of the Reynolds number:

$$
C_d = \frac{2}{\rho \cdot A} \cdot \left(K_{d2} + \frac{k_{d1}}{v} \right) = \frac{2}{\rho \cdot A} \cdot \left(c + \frac{b \cdot l}{\nu \cdot Re} \right).
\tag{26}
$$

Then, from the values of b and c in Table 1 combined with the vehicle data reported before, it is possible to obtain the plot of Figure 7.

Here, additional literature data and CFD (Computational Fluid Dynamics) results are included with some regression lines. The CFD model was implemented through CD-Adapco[35] Star-CCM+® and simulated at the speeds of 10, 25, 75 and 125 km/h. A simulation domain of $25 \times 6 \times 5$ m as in Figure 8(a) was used referring to length, width and height, respectively. The rotation of the wheels was imposed as a boundary condition for the flow as far as the ground movement and no-slip wall condition. Since the model was originally developed to evaluate the effects of internal ventilation on the overall drag (a detailed analysis is planned for future publication), the main bodies inside the fairing were included as far as the air inlet and outlet. The overall domain mesh counts approximately 6E+6 cells. The segregated flow solver with Spalart-Almaras turbulence model converged in 7.6 hours (CPU time 59 hours) on a Dell Precision T7400 workstation with $2\times$ Intel® Xeon® quad-core and 16 GB RAM.

Under hypothesis 3), the estimated dependence of C_d on the speed looks excessive with respect to both literature and simulation trends. Moreover, the power regression on CFD data fits better than the inverse linear one (higher R^2), suggesting that the speed dependence for the drag coefficient could have a different form than the one assumed in the present work. It must be remembered that this qualitative evaluation is based on a first approximation model for C_d as a function of speed, Eq. (26), which is supposed (but not proved) to be better than assuming a fully constant behaviour. This approximation is not able to identify any flow regime transition, critical Re or other effects that could occur at higher speeds. Also, the CFD model used for the comparison is based on a full turbulent model with no capabilities to predict any laminar-turbulent transition. From this perspective, considering the roughly finished junctions
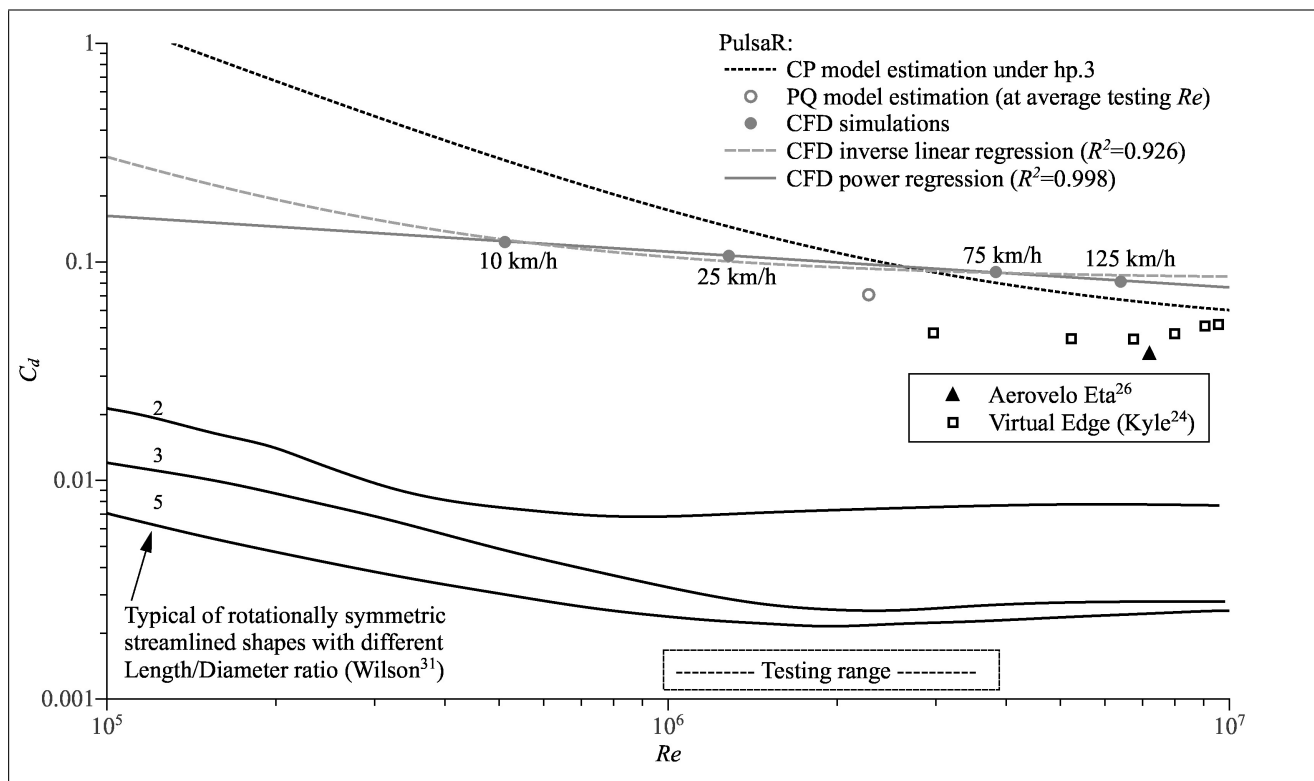
Figure 7. Drag coefficient versus Reynolds number: PQ and CP models, CFD simulations and literature data.

of the tested prototype (i.e. at the border of the front acrylic glass, Figure 1), it is likely that the testing regimes were also rather fully turbulent. This implies that, although a variation of the drag coefficient with the speed can partly produce the estimated linear term, it does not provide a self-sufficient explanation for its overall value. As a consequence, hypothesis 3) is rejected.

Selecting the more suitable model

Since all three hypotheses were rejected, in the specific case study there is no way to obtain a distinct estimation of the force coefficients and this highlights the main disadvantage of the CP model. It is the price to pay for the potentially improved predictive reliability given by the introduction of speed-dependent force coefficients.

Advantages and disadvantages of the PQ and CP models are summarized in Figure 9. It follows that the selection of the appropriate coast-down model for a specific case study should be based on the overall purpose of the analysis:

- if the aim is to compare different vehicles or configurations within a specific range of speeds, the PQ model gives a more direct and clear tool by providing distinct quantification of the air-drag and of the rolling-resistance contributions;
- if the aim is to obtain a predictive evaluation or comparison of the required power beyond the available testing range, the CP model is expected to provide a more reliable result by including first approximation models for the speed-dependent force coefficients.
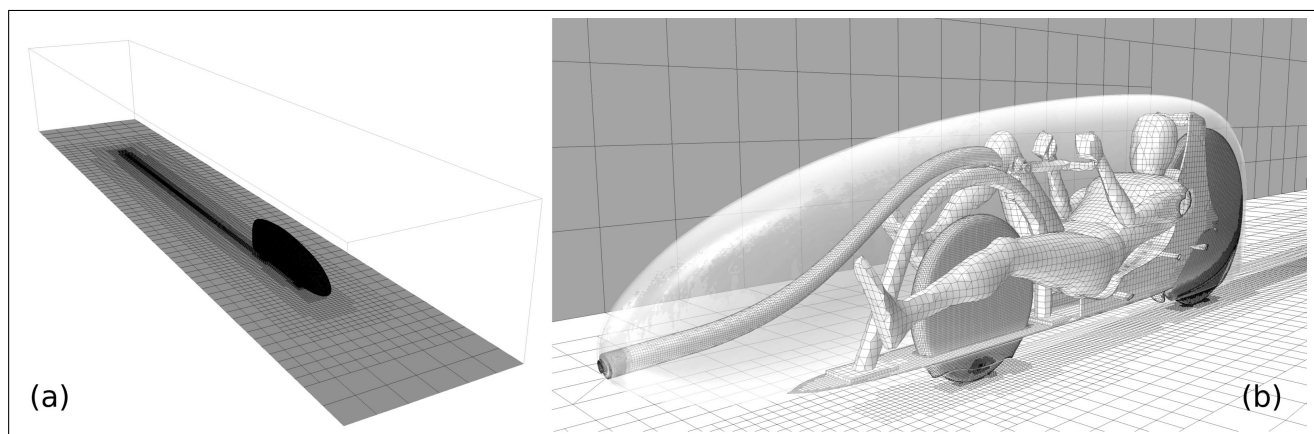

Figure 8. CFD model volumetric mesh: overall domain (a) and vehicle internal details (b).

Figure 9. Comparison scheme for the PQ and the CP models.

Conclusions

This work started from the need of a coast-down model overcoming the assumption of speed-independent force coefficients. The aim was to obtain a model providing more reliable prediction of the power required beyond the testing speed range, which is often restricted by external boundary conditions for top-speed HPVs. A complete polynomial model for the equation of motion was then considered, developed and applied to a case study.

From the developed model, the obtained results and the discussion, it was possible to point out that:

- due to its basic assumptions, the PQ model provides distinct averaged values for the resistive forces within a defined range of speed;
- the CP model includes a speed-dependent linear term that accounts for three potential sources: the freehub losses, a linear dependence on speed for the coefficient of rolling-resistance and an inverse linear dependence on speed for the coefficient of drag;
- fitting comparison on a case study showed that the additional term of the CP model is not useless (both R^2 and $\bar{R}^2$ are increased) and that the difference between the two models becomes significant when predicting the power required above 100 km/h;
- as a side effect for its potentially improved reliability in prediction, the CP model does not allow a distinct estimation for the retarding forces, due to the presence of a mixed contribution in the linear term.

Eventually, by neglecting the freehub contribution, it would be possible to assume one of the obtained CFD regressions (Figure 7) for the C_d in order to estimate the residual contribution for the C_{rr} dependence on the speed. However, considering the number of assumptions and approximations that this process would involve, it is not considered a reliable way to obtain an accurate distinctive evaluation of the retarding forces.

A validation of the CP model will be possible by collecting data at higher speeds, possibly completed with a power meter. Moreover, an interesting development for future testing with this kind of vehicles is the possibility to accurately log deceleration data instead of (or beside) the speed. By overcoming the need for solving the differential equation, this would allow the exploration of a larger amount of possibilities for the equation of motion in order to achieve an adequate predictive reliability.

References

1. Candau R, Grappe F, Ménard M et al. Simplified deceleration method for assessment of resistive forces in cycling. *Med Sci Sports Exerc* 1999; 31(10): 1441–1447.
2. Wehrbein WM. Collecting and recording bicycle speed data by cbl. *Phys Teach* 2003; 41(4): 243–244.
3. Underwood L and Jermy M. Mathematical model of track cycling: the individual pursuit. *Procedia Eng* 2010; 2(2): 3217 – 3222. DOI:10.1016/j.proeng.2010.04.135.
4. Hennekam W and Bontsema J. Determination of fr and kd from the solution of the equation of motion of a cyclist. *Eur J Phys* 1991; 12(2): 59.
5. Hennekam W and Govers M. The freewheeling cyclist. *Phys Educ* 1996; 31(5): 320–328.
6. Di Giovine C, Cooper R and Dvornak M. Modeling and analysis of a manual wheelchair coast down protocol. In *Engineering in Medicine and Biology Society, 1997. Proceedings of the 19th Annual International Conference of the IEEE*, volume 5. pp. 1888–1891 vol.5. DOI:10.1109/IEMBS. 1997.758702.
7. Fuss FK. Influence of mass on the speed of wheelchair racing. *Sports Eng* 2009; 12(1): 41–53. DOI:10.1007/ s12283-009-0027-2.
8. Webb AP, Taunton DJ, Hudson DA et al. Repeatable techniques for assessing changes in passive swimming resistance. *Proc IMechE Part P: Journal of Sports Engineering and Technology* 2015; 229(2): 126–135. DOI:10.1177/1754337114562875.
9. Federolf P and Redmond A. Does skate sharpening affect individual skating performance in an agility course in ice hockey? *Sports Eng* 2010; 13(1): 39–46. DOI:10.1007/ s12283-010-0050-3.
10. Poirier L, Lozowski EP, Maw S et al. Experimental analysis of ice friction in the sport of bobsleigh. *Sports Eng* 2011; 14(2): 67–72. DOI:10.1007/s12283-011-0077-0.
11. Petrushov V. Coast down method in time-distance variables. *SAE Technical Paper* 1997; N.970408. DOI:10.4271/970408.
12. Petrushov V. Improvement in vehicle aerodynamic drag and rolling resistance determination from coast-down tests. *Proc*

IMechE Part D: Journal of Automobile Engineering 1998; 212(5): 369–380. DOI:10.1243/0954407981526037.

13. Ivens J. The rolling resistance of some 13 inch tires and the correlation between rig and road. *SAE Technical Paper* 1987; 870422. DOI:10.4271/870422.

14. Evans EM and Zemroch PJ. Measurement of the aerodynamic and rolling resistances of road tanker vehicles from coast-down tests. *Proc IMechE Part D: Journal of Automobile Engineering* 1984; 198(3): 211–218. DOI:10.1243/PIME_PROC_1984_198_147_02.

15. Stepwise coastdown methodology for measuring tire rolling resistance. Surface Vehicle Recommended Practice J2452, SAE International, 1999.

16. Road load measurement using onboard anemometry and coastdown techniques. Surface Vehicle Recommended Practice J2263, SAE International, 2012.

17. Roussillon G. Contribution to accurate measurement of aerodynamic drag on a moving vehicle from coast-down tests and determination of actual rolling resistance. *J Wind Eng Ind Aerodyn* 1981; 9(1-2): 33–48. DOI:10.1016/0167-6105(81)90076-3.

18. Martin JC, Milliken DL, Cobb JE et al. Validation of a mathematical model for road cycling power. *J Appl Biomech* 1998; 14(3): 276–291.

19. Di Prampero P, Cortili G, Mognoni P et al. Equation of motion of a cyclist. *J Appl Physiol* 1979; 47: 201.

20. Drory A and Yanagisawa M. Predictive mathematical model of time saved on descents in road cycling achieved through reduction in aerodynamic drag area. *Proc IMechE Part P: Journal of Sports Engineering and Technology* 2012; 226(2): 152–160. DOI:10.1177/1754337112440643.

21. Lukes R, Hart J and Haake S. An analytical model for track cycling. *Proc IMechE Part P: Journal of Sports Engineering and Technology* 2012; 226(2): 143–151. DOI:10.1177/1754337111433242.

22. Website http://recumbents.com/wisil/whpsc2016 - Accessed on April 5th, 2016.

23. Website http://www.ihpva.org - Accessed on April 5th, 2016.

24. Kyle CR and Weaver MD. Aerodynamics of human-powered vehicles. *Proc IMechE Part A: Journal of Power and Energy* 2004; 218(3): 141–154. DOI:10.1243/095765004323049878.

25. Epema H, van den Brand S, Gregoor W et al. Bicycle design: A different approach to improving on the world human powered speed records. *Procedia Eng* 2012; 34: 313 – 318. DOI:10.1016/j.proeng.2012.04.054.

26. Website http://www.aerovelo.com - Accessed on April 5th, 2016.

27. Popov A, Cole D, Cebon D et al. Energy loss in truck tyres and suspensions. In Froehling R (ed.) *Vehicle System Dynamics Supplement*. 33, pp. 516–527.

28. Popov A, Cole D, Winkler C et al. Laboratory measurement of rolling resistance in truck tyres under dynamic vertical load. *Proc IMechE Part D: Journal of Automobile Engineering* 2003; 217(12): 1071–1079. DOI:10.1243/09544070360729419.

29. Kyle C and Burke E. Improving the racing bicycle. *Mech Eng* 1984; 106(9): 34.

30. Grappe F, Candau R, Belli A et al. Aerodynamic drag in field cycling with special reference to the obree's posture. *Ergonomics* 1997; 40: 1299.

31. Wilson D. *Bicycling Science*. 3rd ed. MIT Press, 2004. (Fig. 5.8, page 185).

32. Munson B, Young D, Okiishi T et al. *Fundamentals of fluid mechanics*. 6th ed. Wiley, 2009. (Fig. 9.22, page 502).

33. Vasilief I. Website http://www.qtiplot.com - Accessed on April 5th, 2016.

34. Theil H. *Economic forecasts and policy*. 2nd ed. Contributions to economic analysis, North-Holland Pub. Co., 1961.

35. Website http://www.cd-adapco.com/products/star-ccm - Accessed on April 5th, 2016.

Appendix I

Notation

a, b, c	Generic polynomial coefficients
c_{dv}	Inverse linear factor for the speed-dependent aerodynamic drag coefficient
c_{rv}	Linear factor for the speed-dependent coefficient of rolling-resistance
f_h	Linear factor for the speed dependence of the freehub retarding force on the speed
f_{rv}	Linear factor for the speed-dependent part of the rolling-resistance force
k_{d1}	Linear coefficient of the speed-dependent aerodynamic drag factor
l	Length of the vehicle
m	Mass of the vehicle
t	Time variable
v	Velocity
v_0	Initial velocity at the beginning of the coast-down
A	Frontal area of the vehicle
C_d	Overall aerodynamic drag coefficient
C_{d0}	Speed independent part of the aerodynamic drag coefficient
C_{r0}	Speed independent part of the coefficient of rolling-resistance
C_{rr}	Overall coefficient of rolling-resistance
F_d	Overall aerodynamic drag force acting on the vehicle
F_{dv1}	Portion of the drag resistance with linear dependence on the speed
F_{dv2}	Portion of the drag resistance with quadratic dependence on the speed
F_r	Overall rolling-resistance force acting on the vehicle
F_{r0}	Speed independent part of the rolling-resistance force
F_{rv}	Speed dependent part of the rolling-resistance force
F_{hub}	Resistive force given by the freehub
N	Ground normal force (the gravitational load if the aerodynamic lift force can be neglected)
K_d	Overall aerodynamic drag factor
K_{d2}	Quadratic coefficient of the speed-dependent aerodynamic drag factor
P_p	Mechanical power at the pedals
P_w	Mechanical power at the wheel
Re	Reynolds Number
β, δ, τ	Parameters of the condensed form for the solution of the differential equation of motion
η	Transmission efficiency (mechanical power at the wheel over mechanical power at the pedals)
ϕ	Phase factor
ρ	Air density
ν	Air kinematic viscosity